Linc01105 acts as an oncogene in the development of neuroblastoma

MUJIE YE[1,2], JING MA[3], BAIHUI LIU[1,2], XIANGQI LIU[1,2], DUAN MA[3,4] and KUIRAN DONG[1,2]

[1]Department of Pediatric Surgery, Children's Hospital of Fudan University; [2]Key Laboratory of Neonatal Disease, Ministry of Health; [3]Shanghai Key Lab of Birth Defect, Children's Hospital of Fudan University, Shanghai 201102; [4]Key Laboratory of Metabolism and Molecular Medicine, Ministry of Education, Department of Biochemistry and Molecular Biology, Institute of Biomedical Sciences, Collaborative Innovation Center of Genetics and Development, School of Basic Medical Sciences, Fudan University, Shanghai 200032, P.R. China

Received April 1, 2019; Accepted July 15, 2019

DOI: 10.3892/or.2019.7257

Abstract. Previous research from our group revealed that the long coding RNA (lncRNA) linc01105 is associated with neuroblastoma proliferation and apoptosis, and that its expression is correlated with the International Neuroblastoma Staging System stage. The purpose of the present study was to investigate the functions of Linc01105 in neuroblastoma. Lentivirus-mediated linc01105 knockdown was performed in the neuroblastoma cell line SH-SY5Y. The expression levels of linc01105 and of other associated genes were measured by reverse transcription-quantitative PCR. Cell Counting Kit-8 assay and flow cytometry were used to determine cell viability and apoptosis. The levels of proteins were detected using western blot analysis. Bioinformatics analysis and luciferase reporter assays were used to examine the relationship between linc01105, miR-6769b-5p and vascular endothelial growth factor A (VEGFA). Angiogenesis ability was measured using a tube formation assay. The results demonstrated that HIF-1α overexpression promoted the transcription of linc01105 by acting as a transcription factor. Knockdown of linc01105 inhibited neuroblastoma cell proliferation, migration and invasion, and it induced apoptosis. In addition, linc01105 affected the expression of p53 and Bcl-2 family proteins and activated the caspase signaling pathway. Further functional experiments revealed that linc01105 promoted the expression of the miR-6769b-5p target gene VEGFA by acting as a sponge of miR-6769b-5p. In conclusion, linc01105 may contribute to neuroblastoma tumorigenesis and development. The present findings indicated that the interplay between the p53/caspase pathway and the linc01105/miR-6769b-5p/VEGFA axis may have important roles in the development of neuroblastoma.

Correspondence to: Professor Kuiran Dong, Department of Pediatric Surgery, Children's Hospital of Fudan University, 399 Wanyuan Road, Shanghai 201102, P.R. China
E-mail: kuirand@hotmail.com

Professor Duan Ma, Shanghai Key Lab of Birth Defect, Children's Hospital of Fudan University, 399 Wanyuan Road, Shanghai 201102, P.R. China
E-mail: duanma@fudan.edu.cn

Key words: long non-coding RNA, neuroblastoma, competing endogenous RNA

Introduction

Neuroblastoma (NB) is the most common extracranial solid tumor in children and is responsible for 10% of the mortality resulting from all pediatric tumors (1,2). The prognosis of many children's malignant tumors has improved by effective treatments. However, high-risk NB remains intractable, with merely 40% of patients achieving long-term survival despite the availability of multiple therapeutic methods (3,4). The tumorigenesis and progression of NB is reported to be complex, and is influenced by both the external environment and internal genetic factors (4,5). Early accurate diagnosis and timely intervention is important to improve prognosis. Therefore, further research investigating the biological targets and underlying molecular mechanisms is essential for improving the diagnosis and therapy of NB (6).

Long non-coding RNAs (lncRNAs) are generally defined as RNA transcripts that are >200 nt with no protein products (7-9). Non-coding RNAs, once considered as transcriptional waste, are actually a part of the regulatory network of transcriptional and post-transcriptional processes (1,10,11). They are ubiquitously expressed in mammalian genomes, and participate in the regulation of numerous biological processes, including DNA methylation, chromatin remodeling, transcription regulation and translation (10,12). It is reported that several lncRNAs are closely linked to NB initiation and progression, and involved in a variety of tumor-associated biological processes (13,14), such as cancer susceptibility 15 (CASC15) (15), MYCN upstream transcript (lncUsMycN) (16) and ETS1 antisense RNA 1 (pancEts-1) (17).

In our previous study, genome-wide lncRNA analysis was performed to detect NB-associated lncRNAs. Linc01105 was identified as differentially expressed between NB and normal adrenal gland tissues. It was also demonstrated that upregulation of linc01105 in NB was correlated with the International Neuroblastoma Staging System (INSS) stage (14). The present study found that hypoxia inducible factor-1α (HIF-1α) may bind at the linc01105 promoter to activate its transcription. In addition, linc01105 knockdown significantly suppressed proliferation and induced apoptosis via the p53/caspase signaling pathway. Furthermore, it is well established that, lncRNAs can act as microRNA (miRNA) sponges, and thus regulate their ability to target mRNAs (18,19). In the present study, it was demonstrated that linc01105 may inhibit tumor angiogenesis via the linc01105/miR-6769b-5p/vascular endothelial growth factor A (VEGFA) network.

Materials and methods

Human tissues and NB cell line. Human NB and adjacent normal adrenal gland tissues were collected from patients who underwent surgery between January 2011 and January 2017 in the Children's Hospital of Fudan University, Shanghai, China. Tumor tissues were diagnosed as NB by the pathology department and all patients were stage III/IV according to INSS. For the present study, 32 patients were enrolled,18 boys and 14 girls. The age of the patients ranged from two months to ten years. Informed consent was acquired from every patient's legal guardians. This study was approved by the Institute Research Ethics Committee at the Children's Hospital of Fudan University.

The NB cell line SH-SY5Y and SK-N-BE (2), the human umbilical vein endothelial cells (HUVECs) and 293T cells were obtained from the Cell Bank of Type Culture Collection of the Chinese Academy of Sciences in Shanghai. CHLA15, LA-N-5, and CHLA136 were gifts from professor Li Kai's lab of FuDan University. The SH-SY5Y and SK-N-BE (2) cells were cultured in DMEM/F12 (Biological Industries) with 10% fetal bovine serum (Biological Industries) in a humidified incubator with 5% CO_2 at 37˚C. HUVEC, 293T, and other NB cell lines(CHLA15, LA-N-5, and CHLA136 cells) were cultured in DMEM with 10% FBS (both Gibco; Thermo Fisher Scientific, Inc.). All cell culture dishes and culture plates were purchased from Hangzhou Xinyou Biotechnology Co., Ltd, China.

Nuclear and cytoplasmic extract preparation. Cells were grown to 90-100% confluency. Pre-cooled PBS was used to wash the cells twice. Cytoplasmic extraction buffer (0.5 ml; Invent Biotechnologies, Inc.) was then added to the cells, and set on ice for 5 min. The lysates were transferred to tubes and mixed rigorously for 15 sec. After centrifuging at 12,000 x g for 5 min at 4˚C, TRIzol was added to the nuclear (pellet) and cytoplasmic fragments (supernatant) for RNA extraction.

Reverse transcription-quantitative PCR (RT-qPCR). Total RNA was extracted using TRIzol reagent (Takara Bio, Inc.) and cDNA was synthesized using a cDNA Reverse Transcription kit (Takara Bio, Inc.). qPCR reactions were performed using SYBR Green PCR Master Mix (Takara Bio, Inc.) on the Step One Real-Time PCR system. The PCR program was: 94˚C for 10 min, 40 cycles of 94˚C for 60 sec and 60˚C for 15 sec. GAPDH was used as internal control. Data was analyzed using GraphPad software (GraphPad Software, Inc.) and relative fold changes in expression were calculated using the formula $2^{-\Delta\Delta Cq}$ (20). The following primer sequences were used in this study: Linc01105, forward 5'-TGTGCCATTCCATGTTATA-3' and 5'-TTGAGGCTGAAGACCAAA-3; and GAPDH, forward 5'-GGAGCGAGATCCCTCCAAAAT-3' and reverse 5'-GGC TGTTGTCATACTTCTCATGG-3'. U1 and actin were used as controls for the nuclear and the cytoplasmic extracts, respectively, and their primes were: U1, forward 5'-GACGGGAAA AGATTGAGCGG-3' and reverse 5'- GCCACGAAGAGAGTC TTGAAGG-3'; actin, forward 5'-CATGTACGTTGCTATCCA GGC-3' and reverse, 5'-CTCCTTAATGTCACGCACGAT-3'.

To quantitatively measure miRNAs, the All-in-OneTM miRNA qRT-PCR Detection kit (GeneCopoeia, Inc.) was used. The experimental procedure included two major steps. Firstly, single-step cDNA synthesis was performed. Poly-A polymerase was used to add poly-A tails to the 3' end of miRNAs, and M-MLV RTase was used simultaneously, with a unique oligodT adaptor primer, to reverse transcribe the miRNA. Secondly, qPCR detection was performed. The All-in-OneTM miRNA qRT-PCR Mix, containing SYBR Green, specifically detects the reverse transcribed miRNA. The miR-6769b-5p-specific primer (cat. no. HmiRQP3816) and the U6 control primer (cat. no. HmiRQP9001) were purchased from GeneCopoeia, Inc.

Construction of shRNA and stable transfected cell lines. Linc01105 shRNA plasmids were designed and constructed by Genomeditech Co., using the pGMLV-SC5 RNAi vector. The control target sequence was 5'-TTCTCCGAACGT GTCACGT-3'. Three different shRNA target sequences were designed as follows: sh1, 5'-GCTCAGGAGAAAGAG CAAATG-3'; sh2, 5'-GCCTGCTGAGAAGGCTCATCT-3'; and sh3, 5'-GCAGCAACTCCTGTGCATGT-3'. Purified, endotoxin-free lentiviral vector and its auxiliary packaging vector plasmids were co-transfected into 293T cells (Cell Bank of Type Culture Collection of the Chinese Academy of Sciences) using the HG transgene reagent (Genomeditech Co.) for 10-12 h. Enhancing buffer (Genomeditech Co.) was added, and the medium was replaced with fresh medium after 8 h. After 48 h of incubation, the supernatant of the cell line, containing the lentiviral particles, was collected and concentrated to obtain a high titer of lentivirus concentrate, with a final virus titer of $5x10^8$ transduction units/ml. SH-SY5Y cells were infected with different shRNA-expressing lentivirus, and stable infected cells were acquired following puromycin selection.

Cell proliferation and viability assay. Cell proliferation and viability were detected using the Cell Counting Kit-8 assay (Yeasen Biotechnology Co., Ltd.) and the cell viability kit (Beyotime Institute of Biotechnology), according to the suppliers' protocols. Cells were cultured in a 96-well plate at a concentration of 2,000 cells per well in 100 μl medium. The Cell-Light EdU DNA cell proliferation kit (Guangzhou RiboBio Co., Ltd.) was also used to assess cell proliferation. For the EdU assay, 10,000 cells were seeded in 24-well plates.

Cells were cultured for 2 h with 50 μM EdU, then 4% formaldehyde was used to fix the cells for 20 min at room temperature. Cells were permeabilized with 0.5% Triton X-100 for 10 min, stained with 200 μl of Hoechst 33342 for 30 min, and visualized under a fluorescent microscope.

Cell apoptosis assay. After digestion with EDTA-free trypsin, cells were collected and washed twice with pre-cooled PBS. Cells (10^6) were transferred into 5 ml flow tubes. Then, 5 μl of Annexin V-APC and 10 μl of 7-AAD (Yeasen Biotechnology Co., Ltd.) were added on the cells in the dark at room temperature for 15 min. Apoptosis rates (percentages of Q2+Q3) were then analyzed by flow cytometry (BD Celesta; Beckman Coulter, Inc.) within 1 h.

Cell migration and invasion assay. Twelve-well culture plates with 8 μm micropore inserts were used for cell migration and invasion assays. Cells were serum-starved for 24 h prior to the assays. For the migration assay, $2x10^5$ NB cells were placed into the upper wells in DMEM/F12 without FBS for 24 h. For the cell invasion assay, the upper side of the insert was coated with Matrigel (BD Biosciences), and $4x10^5$ NB cells were placed into the upper wells without FBS for 24 h. The cells on the lower sides of the inserts were then fixed with 4% paraformaldehyde for 10 min and stained with 0.1% crystal violet for 30 min. Five fields were randomly selected and captured using a light microscope (Olympus Corporation), and the average count of the five fields was calculated.

Wound healing assay. Cells ($1x10^5$) were seeded in the two wells of culture inserts (Ibidi GmbH). After the cells were attached and the insert was removed, a standard gap was left between the cells. The gap closure was observed at x100 magnification and photographs were captured using light microscopy at 0, 6, 12 and 24 h. Image J (National Institutes of Health) was used to measure the gap width.

Caspase-3 activity assay. Caspase-3 activity was detected using the caspase-3 activity kit (Beyotime Institute of Biotechnology). According to the manufacturer's instructions, cells were mixed with buffers containing caspase-3 substrate and incubated at 37˚C for 2 h. Samples were the detected at 450 nm using a plate reader.

Western blotting. Cell proteins were extracted by lysis buffer (Beyotime Institute of Biotechnology), and western blotting was performed with standard procedures (21). Briefly, after blocking, the membranes were incubated with primary antibodies at 4˚C overnight. The primary antibodies were as follows: Anti-BCL2 (cat. no. 60178; 1:2,000; ProteinTech Group, Inc.), anti-Bax (cat. no. 50599; 1:2,000; ProteinTech Group, Inc.), anti-caspase-3 (cat. no. 19677; 1:500; ProteinTech Group, Inc.), anti-caspase-9 (cat. No 10380; 1:500; ProteinTech Group, Inc.), anti-active caspase-3 (cat. no. F021507; 1:500; Abways Technology), anti-cleaved caspase-9 (cat. no. F016210; 1:500; Abways Technology), anti-p53 (cat. no. F024201; 1:500 Abways Technology), anti-poly (ADP-ribose) polymerase (PARP; cat. no. AP102-1; 1:1,000; Beyotime Institute of Biotechnology), anti-VEGFA (cat. no 19003; 1:1,000; ProteinTech Group, Inc.), and anti-tubulin (cat. no. ab210797; 1:1,000; Abcam). After washing with TBS/0.5% Tween 20 three times, the membranes were incubated with the relevant secondary antibody (goat anti-rabbit cat. no. CW0156, 1:2,000; or goat anti-mouse cat. no. CW0110, 1:5,000; both ComWin Biotech Co., Ltd.) for 1 h at room temperature. The protein signals were detected using an enhanced chemiluminescence substrate (EMD Millipore).

Transient transfections. Cells (10^4) were seeded in a 24-well plate one day in advance, and the cell confluence was ~30% at the time of transfection. Small interfering RNA (siRNA) or miRNA mimics or inhibitor (50 pmol) were added to OPTI-MEM (Gibco; Thermo Fisher Scientific, Inc.) to a final volume of 25 μl and mixed well. Then, 1 μl of Lipofectamine 2000 (Thermo Fisher Scientific, Inc.) was added to OPTI-MEM to a final volume of 25 μl. The two solutions were then thoroughly mixed at room temperature for 15 min. The 50 μl of transfection complex was added to cells in 0.45 ml media, and incubated for 48 h. The sequences were as follows: siVEGFA, 5'-GUGCUACUGUUUAUCCGUA-3'; negative control (NC) siNC, 5'-UUCUCCGAACGUGUCACGU-3'; miR-107 mimics, 5'-GCCUUCUGACUCCAAGUCCAGU-3', miR-378a-3p mimics, 5'- UGAUAGCCCUGUACAAUGCUGCU-3', miR-6769b-5p mimics, 5'-UCUACUCUUUCUAGGAGGUUGUGA-3'; mimics NC, 5'-GCACUUCUCCUCCCCACCCACCA-3'; miR-6769b-5p inhibitor, 5'-GCACUUCCUCCCCACCCACCA-3'; and inhibitor NC, 5'-UCACAACCUCCUAGAAAGAGUAGA-3'. HIF-1a and VEGFA plasmids (both in pCDH vector) were purchased from Shanghai Generay Biotech Co, Ltd, and transfected (4 μg) into cells with Lipofectamine 2000 (Thermo Fisher Scientific, Inc.). After 48 h of transfection, subsequent experiments were performed.

Luciferase assays. 293T cells were seeded in 24-well plates. When cells reached 75-85% density, they were transfected with luciferase reporter plasmids containing the 3' untranslated region (UTR) of VEGF or the promoter of linc01105 (both constructed by Generay Biotech Co., Ltd.) using Lipofectamine 2000, according to the manufacturer's instructions. After 48 h, luciferase activity (Dual Luciferase Reporter Gene Assay kit; Yeasen Biotechnology Co., Ltd) was measured using a microplate reader and *Renilla* luciferase activity was used for normalization.

Tube formation assay. HUVECs ($5x10^3$) were seeded into a 96-well plate that was pre-coated with Matrigel (BD Biosciences). Conditioned media (CM) supernatant from the stable-infected SH-SY5Y cells were added to the HUVEC cells. A VEGFA antibody (cat. no. 19003; 1:500; ProteinTech Group, Inc.) was used for 6 h pre-treatment in the tube formation assay, as indicated. After 6 h of incubation, tube formation was observed using phase-contrast light microscopy.

Database used for exploring miRNAs. To determine whether linc01105 functions as a miRNA sponge, first the DIANA-LncBase database was used to search for potential miRNA recognition elements on linc01105 (http://diana.imis.athena-innovation.gr). The search term was linc01105, and multiple miRNAs were predicted to bind. The CircNet database (http://circnet.mbc.nctu.edu.tw) was used to search for miRNAs that may bind with VEGFA. Finally, three miRNAs, miR-107,

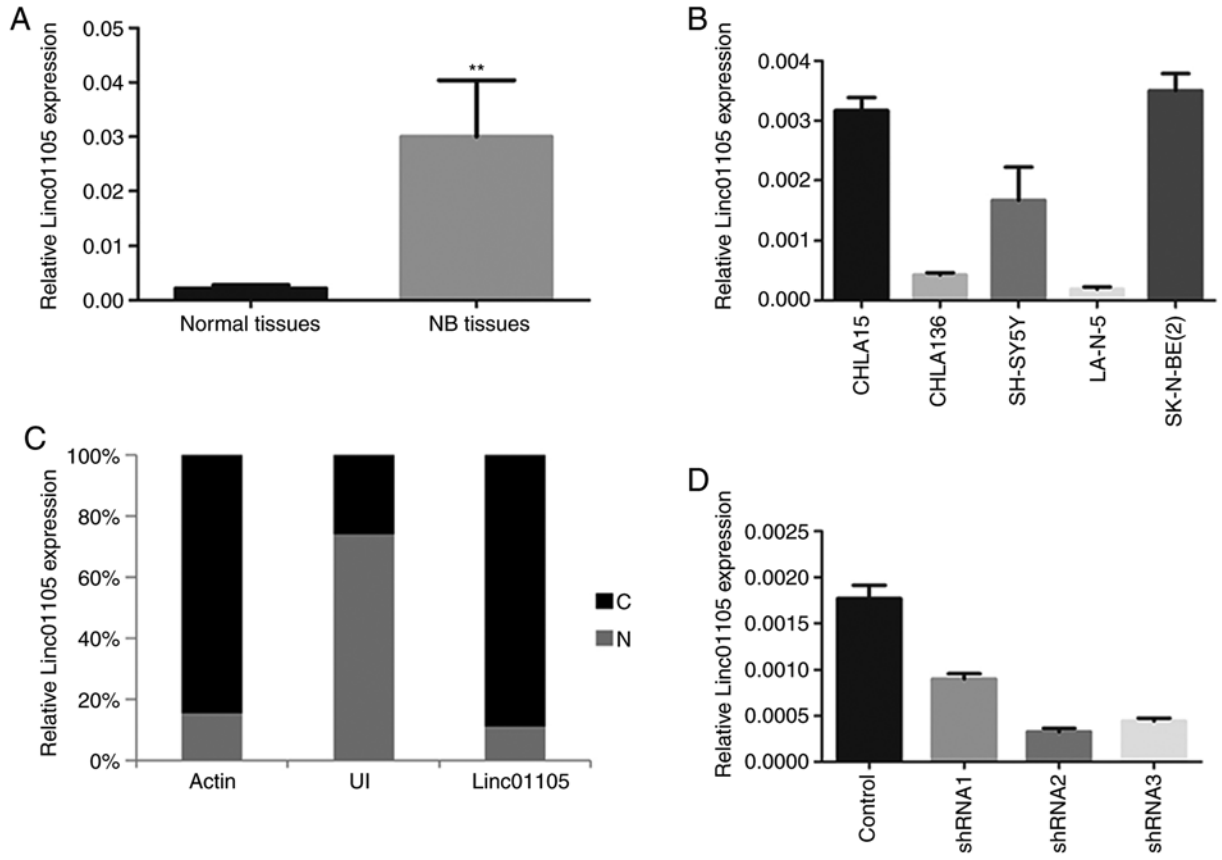

Figure 1. Expression and cellular localization of linc01105 in NB. (A) Linc01105 expression levels in NB and normal tissues were measured by RT-qPCR. (B) Linc01105 expression levels in CHLA-15, CHLA-136, SH-SY5Y, L-A-N-5 and SK-N-BE(2) cells were measured by RT-qPCR. (C) Linc01105 expression in nucleal and cytoplasmic extracts of SH-SY5Y. Actin and U1 were used as cytoplasmic and nuclear internal control genes, respectively. (D) Linc01105 levels in SH-SY5Y cells infected with shRNA lentivirus against linc01105 or negative control were evaluated by RT-qPCR. **P<0.01. NB, neuroblastoma; RT-qPCR, reverse transcription-quantitative PCR; C, cytoplasm; N, nucleus; shRNA, short hairpin RNA.

miR-6769b-5p, miR-378a-3p were identified as potential miRNAs that could bind with both linc01105 and VEGFA.

Chromatin immunoprecipitation (ChIP). ChIP assay was performed as described by Morelli *et al* (22). The cells of one 10 cm dish were sonicated 4 times for 10 sec at pre-cooled conditions (Fisher Sonic Dismembrator; Thermo Fisher Scientific, Inc.) and then treated according to the standard protocol. Anti-HIF-1 (cat. no. 39665; Active Motif, Inc.) or control rabbit IgG (cat. no. 294670; Abmart, Inc.) antibodies were used to capture chromatin fragments from cell extracts. PCR was used to amplify the DNA fragment with the antibody and the input DNA was used as control.

Chromatin isolation by RNA purification (CHIRP). Linc01105 antisense DNA (asDNA), β-galactosidase (lacZ) asDNA and linc01105 sense DNA probes were designed using an online probe designer (singlemoleculefish.com). Oligonucleotides were biotinylated at the 3' end with an 18-carbon spacer arm. Cells were collected and subjected to CHIRP, using the method previously described by Chu *et al* (23). GO and KEGG analysis were performed using the DAVID Functional Annotation web-based tool (http://david.ncifcrf.gov).

Statistical analysis. All results are presented as mean ± standard deviation. Results from different groups were compared using the Student's test or one-way ANOVA followed by Turkey multiple comparisons test. Statistical analysis was performed using GraphPad Prism 5 (GraphPad Software, Inc.). P<0.05 was considered to indicate a statistically significant difference.

Results

Expression and localization of linc01105. Linc01105 was significantly upregulated in the 32 NB specimens compared with the matched normal adrenal gland tissues (Fig. 1A). The SH-SY5Y (non-MYCN amplification) cell line was selected as the *in vitro* model for NB in the present study (Fig. 1B), as our previous study had used SK-N-BE (2)C (MYCN amplification) and CHLA15 was too difficult to culture. Nuclear and cytosolic RNA of SH-SY5Y was extracted and detected by RT-qPCR. The differential enrichments of U1 small nuclear RNA and actin were used as controls for the nuclear and the cytoplasmic extracts, respectively. The results demonstrated that linc01105 expression levels were clearly increased in the cytosol relative to the nucleus (Fig. 1C), which suggested that linc01105 was mainly localized in the cytosol and thus may have a key role in post-transcriptional events. In order to investigate the function of linc01105, three individual shRNAs and a negative control shRNA were purchased from Genomditech. Following lentiviral infection, the RT-qPCR results confirmed

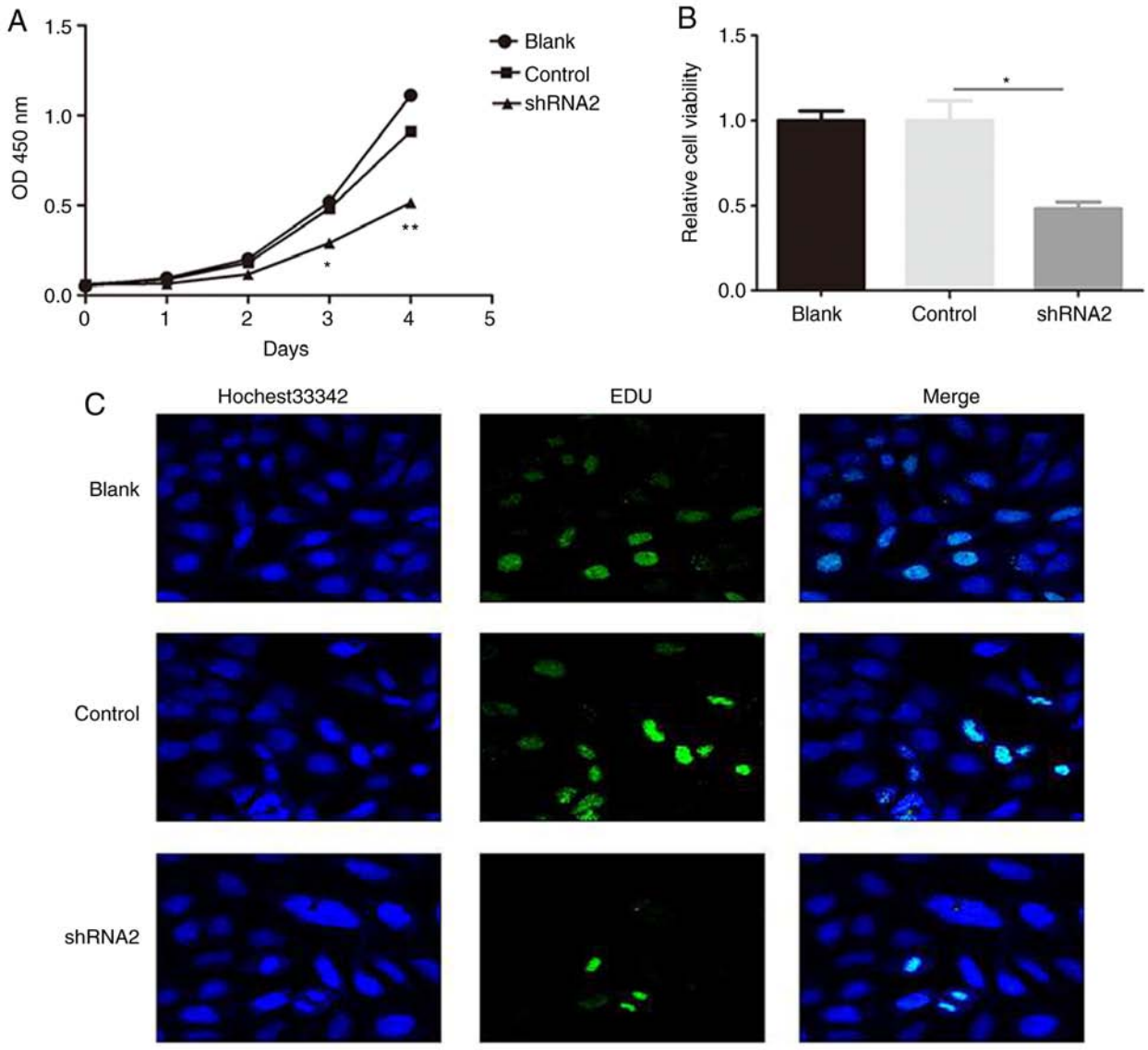

Figure 2. Linc01105 knockdown results in decreased cell proliferation. (A) CCK-8 assay was used to measure neuroblastoma cell proliferation. (B) Cell viability assay was performed. (C) Cell-Light EdU DNA assay was used to further assess cell proliferation. *P<0.05, **P<0.01 compared with control. shRNA, short hairpin RNA.

that shRNA2 had the highest knockdown efficiency, and thus was selected for subsequent experiments (Fig. 1D).

Knockdown of linc01105 inhibits proliferation and viability. To further explore the biological function of linc01105 in NB cells, a shRNA2 stable-infected line was generated in SH-SY5Y cells. A CCK-8 assay was performed to investigate the effect of linc01105 on cell proliferation. Silencing of linc01105 significantly inhibited NB cell proliferation compared with negative control (Fig. 2A). In addition, cell viability was reduced following linc01105 silencing (Fig. 2B). Finally, similar results were observed with the Cell-Light EdU DNA cell proliferation assay (Fig. 2C). Taken together, these results revealed that downregulation of linc01105 may inhibit cell proliferation.

Knockdown of linc01105 contributes to increased apoptosis. Compared with the control group, knockdown of linc01105 induced cell apoptosis, as evidenced by flow cytometry analysis (Fig. 3A). To investigate this further, a caspase-3 activity assay was performed to evaluate the activation of caspase-3 (Fig. 3B). Knockdown of linc01105 resulted in increased caspase-3 activation compared with the control group. Western blot analysis for proteins associated with the Bcl-2 family and the p53/caspase pathway further confirmed that linc01105 knockdown resulted in an obvious apoptotic effect in NB cells (Fig. 3C). Bcl-2 family proteins and the p53/caspase pathway are important regulatory factors of apoptosis (24-26). As shown in Fig. 3C, the expression levels of the antiapoptotic protein Bcl-2 were decreased, while the expression levels of the pro-apoptotic protein Bax were increased following Linc01105 knockdown. Consistent with this, pro-caspase9/3 expression levels were downregulated, while cleaved caspase9/3 and PARP, a marker of caspase3 activation, were upregulated.

Knockdown of linc01105 inhibits migration and invasion. Transwell assays were performed to evaluate the effect of linc01105 knockdown on the migration and invasion of NB

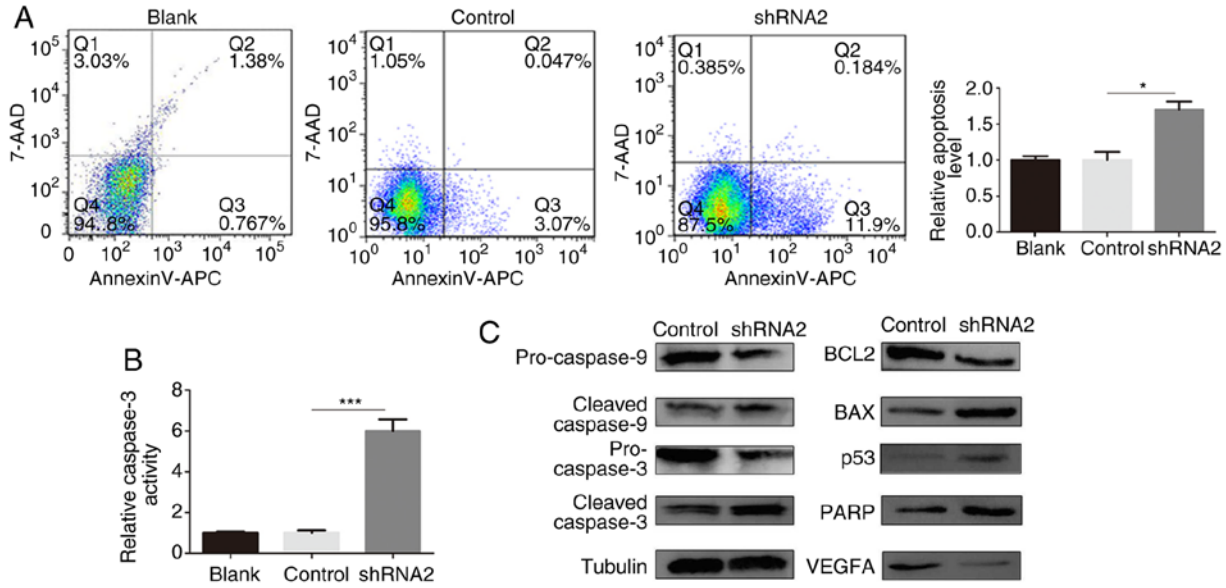

Figure 3. Linc01105 knockdown results in increased cell apoptosis. (A) Annexin V-APC/7-AAD double staining and flow cytometry were used to detect cell apoptosis. (B) Caspase-3 activity assay was performed to evaluate the activation of caspase-3. (C) Expression levels of apoptosis-associated proteins and VEGFA protein were evaluated by western blot analysis. *P<0.05, ***P<0.005 compared with control. APC, allophycocyanin; 7-AAD, 7-aminoactinomycin D; VEGFA, vascular endothelial growth factor A; shRNA, short hairpin RNA; PARP, poly (ADP-ribose) polymerase.

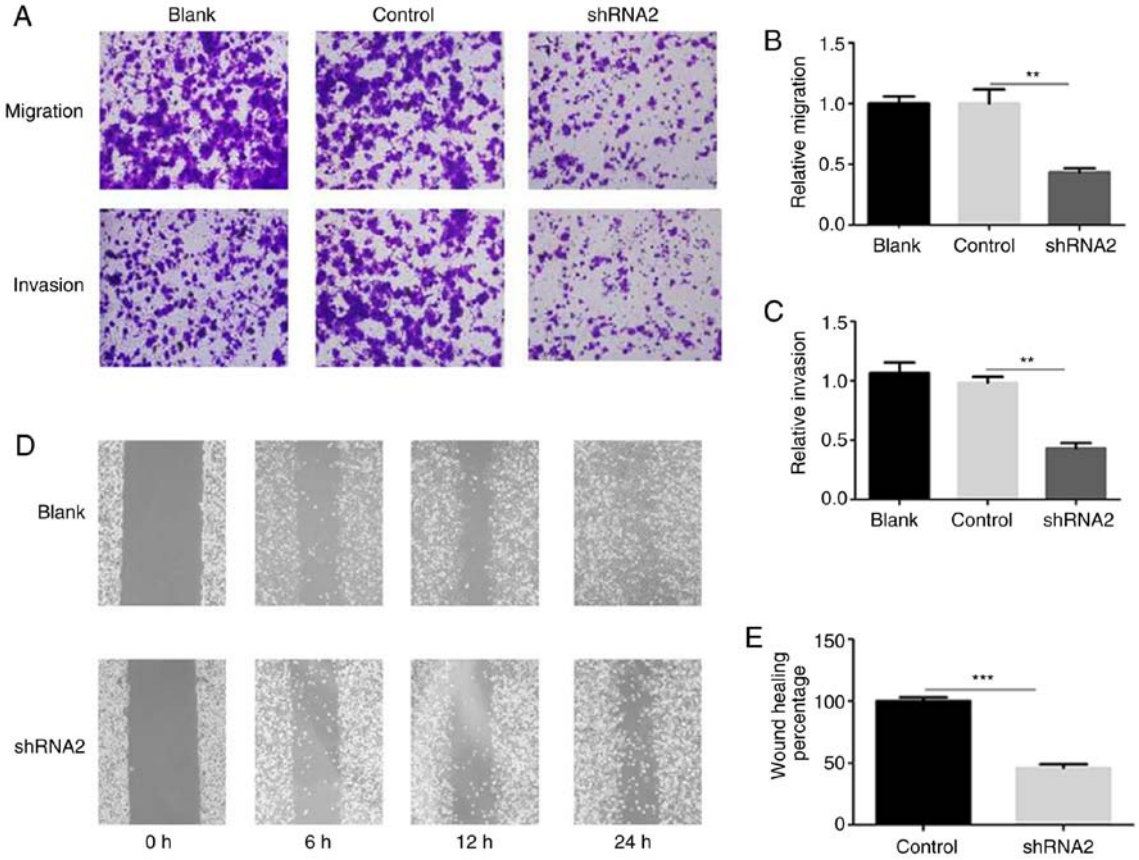

Figure 4. Silencing of linc01105 inhibits migration and invasion in SH-SY5Y cells. (A) Representative images of Transwell migration and invasion assays. (B) Quantification of migration. (C) Quantification of invasion. (D) Representative images and (E) quantification of wound closure assay. **P<0.01, ***P<0.005 compared with control. shRNA, short hairpin RNA.

cells. The results demonstrated that silencing linc01105 significantly inhibited NB cell migration (Fig. 4A and B) and invasion (Fig. 4A and C), compared with the control group. Furthermore, analysis of the wound healing assay indicated that knockdown of linc01105 significantly suppressed NB cell migration (Fig. 4D and E).

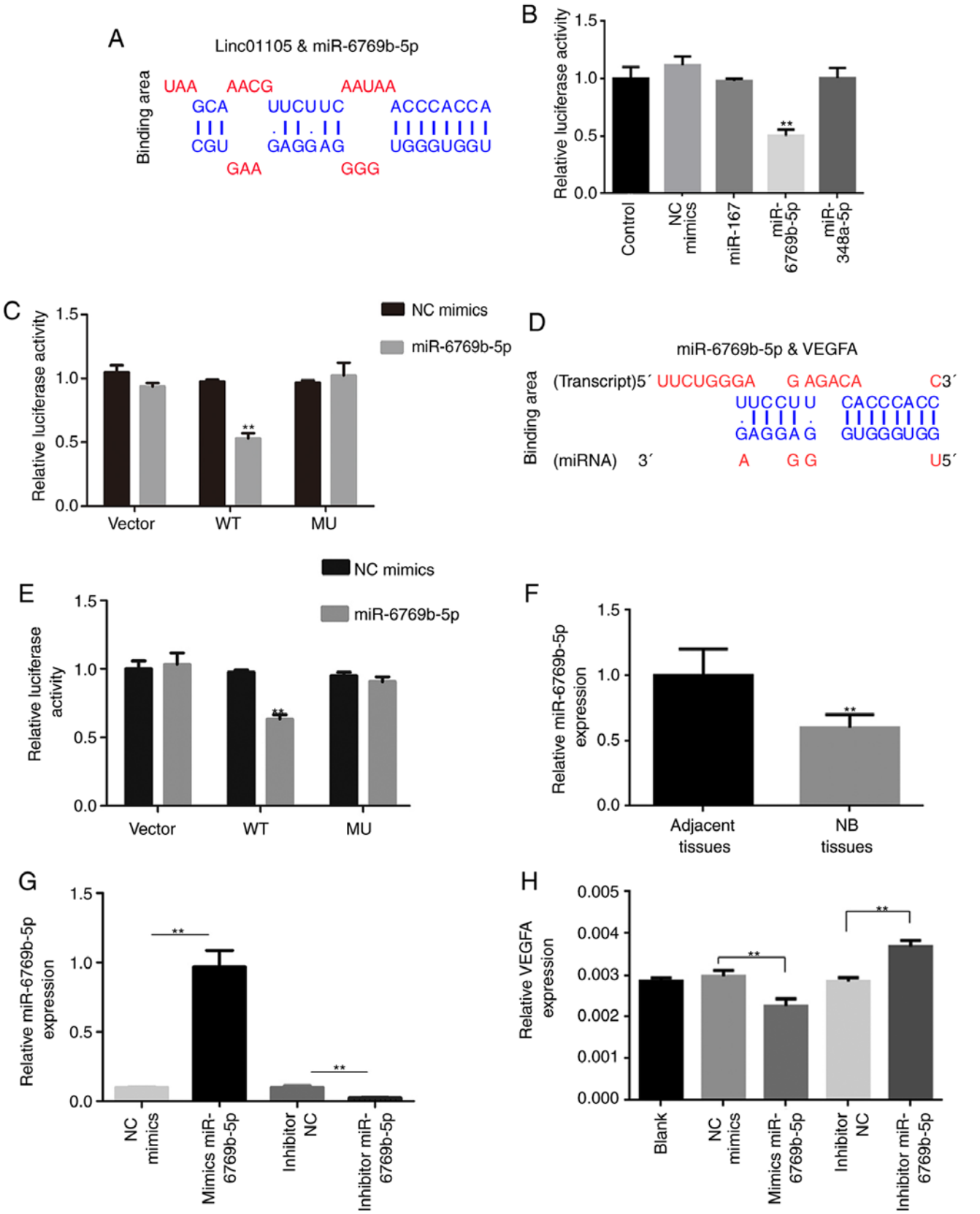

Figure 5. miR-6769b-5p binds to linc01105 and VEGFA in 293T cells. (A) The predicted binding site of miR-6769b-5p and linc01105. (B) The relative luciferase activities of linc01105 following transfection with miR-107, miR-378a-3p and miR-6769b-5p mimics. **P<0.01 compared with NC mimics. (C) The relative luciferase activities of the wild type or mutant linc01105 reporter plasmid following transfection with miR-6769b-5p mimics. **P<0.01 compared with NC mimics. (D) The predicted binding site of miR-6769b-5p and VEGFA. (E) The relative luciferase activities of the wild type or mutant VEGFA 3'UTR reporter plasmid following transfection with miR-6769b-5p mimics. **P<0.01 compared with NC mimics. (F) miR-6769b-5p expression levels in NB and adjacent normal tissues. U6 was used as the internal control gene. **P<0.01 compared with adjacent tissues. (G) Validation of miR-6769b-5p overexpression and knockdown by mimics or inhibitor transfection, respectively. **P<0.01 compared with NC. (H) VEGFA mRNA expression levels following transfection with either miR-6769b-5p mimics, inhibitor or their respective control. **P<0.01 compared with NC. VEGFA, vascular endothelial growth factor A; NC, negative control; UTR, untranslated region; WT, wild type; MU, mutant.

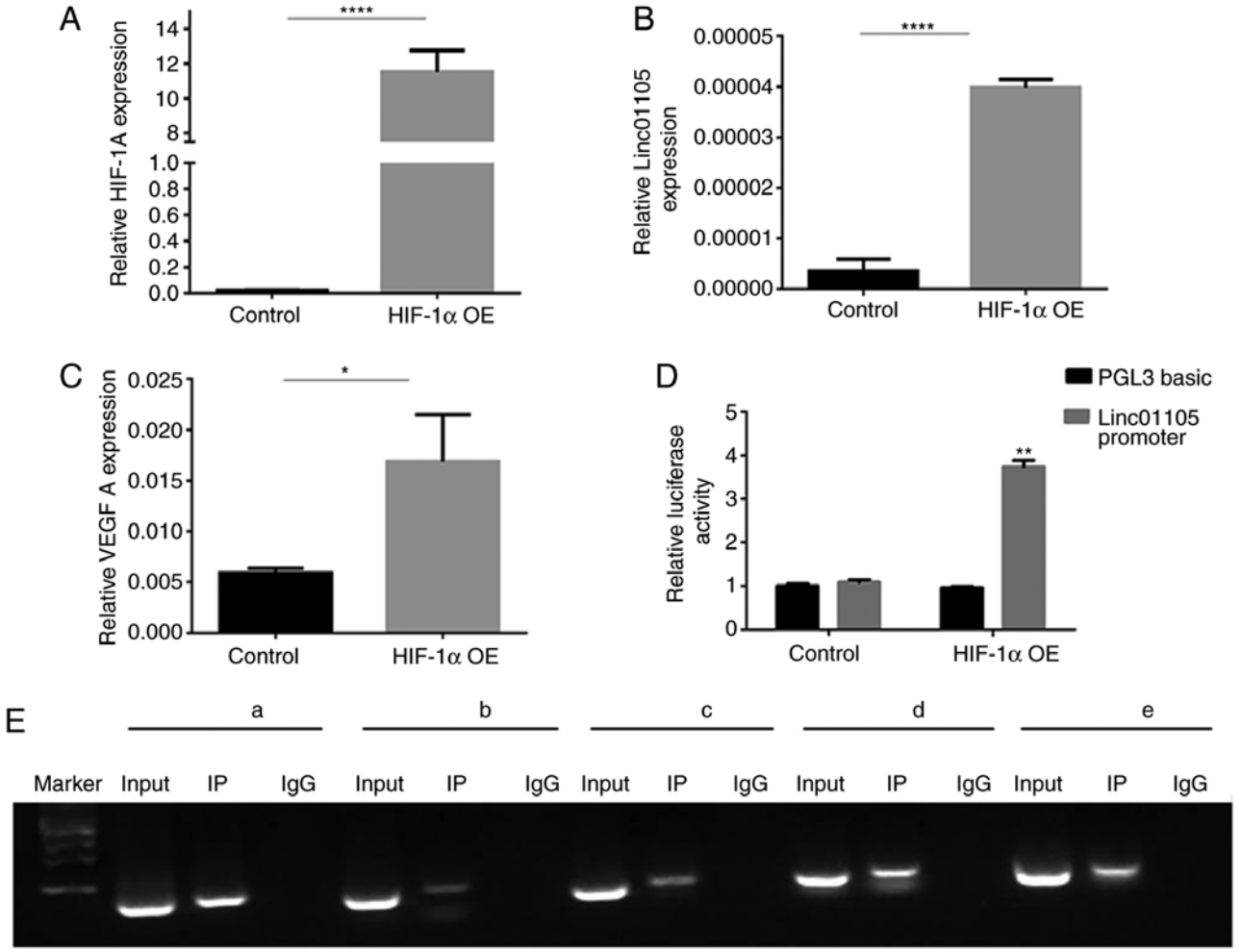

Figure 6. HIF-1α activates the transcription of linc01105. (A) Validation of HIF-1α overexpression in SH-SY5Y cells by transient transfection with a HIF-1α-expressing plasmid. (B) Linc01105 expression levels and (C) VEGFA mRNA expression levels were upregulated following HIF-1α overexpression in SH-SY5Y cells. (D) The relative luciferase activities following co-transfection with a linc01105 promoter reporter plasmid and the HIF1α overexpression plasmid. (E) Chromatin immunoprecipitation assay for HIF-1α and the promoter region of Linc01105. The promoter region fragments are shown as follows: A, 1-400 bp; b, 400-800 bp; c, 800-1,200 bp; d, 1,200-1,600 bp; e, 1,600-2,000 bp. *P<0.05, **P<0.01 and ****P<0.0001. HIF-1α, hypoxia inducible factor-1α; OE, overexpression; IP, immunoprecipitation; IgG, immunoglobulin G.

Linc01105 regulates the expression of miR-6769b-5p targeting VEGFA in NB cells. To explore the mechanism of linc01105 in NB progression, a potential link with VEGFA, a key angiogenic factor involved in NB angiogenesis, was explored. DIANA-LncBase and CirNet database analyses were used to search for potential miRNAs binding with both linc01105 and VEGFA (Fig. 5A and D). miR-107, miR-6769b-5p and miR-348a-3p were identified as potential miRNAs involved in this process. To examine this, the cDNA of linc01105 was cloned into a luciferase reporter plasmid (RLuc-Linc01105-WT). Subsequently, the luciferase reporter plasmid and different miRNA mimics were transfected into 293T cells. Luciferase activity was significantly decreased by miR-6769b-5p mimics transfection (Fig. 5B), but not by the other miRNA mimics tested. To avoid unspecific binding, the miR-6769b-5p binding site of linc01105 and VEGFA was mutated from ACCCACC to TGGGTGG. Transfection of miR-6769b-5p mimics significantly inhibited RLuc-Linc01105-WT activity, but had no effect on RLuc-Linc01105-Mut activity (Fig. 5C). Similar results were observed for the RLuc-VEGFA-WT and RLuc-VEGFA-MU activities (Fig. 5E). Next, the miRNA-6769b-5p expression levels were detected in NB tissues and adjacent normal tissues (Fig. 5F). To further confirm that VEGFA was a target gene of miRNA-6769b-5p, miRNA-6769b-5p mimics and inhibitor were transfected into SH-SY5Y cells (Fig. 5G). The results revealed that miRNA-6769b-5p mimics decreased the expression of VEGFA, while miRNA-6769b-5p inhibitor transfection increased VEGFA expression (Fig. 5H).

HIF-1α activates the expression of linc01105 by acting as a transcription factor. HIF-1α was predicted to bind with the linc01105 promoter region through analysis with the ALGGEN (http://alggen.lsi.upc.es) and JASPAR (http://jaspar.genereg.net) databases. Therefore, a HIF-1α-expressing plasmid was transfected in SH-SY5Y cells (Fig. 6A). The results demonstrated that overexpression of HIF-1α upregulated linc01105 levels (Fig. 6B). VEGFA expression levels were also upregulated following HIF-1α overexpression (Fig. 6C). Subsequently, the linc01105 promoter (2 kb upstream the transcript start site) was cloned into a luciferase gene reporter (RLuc-Linc01105-promoter-WT)

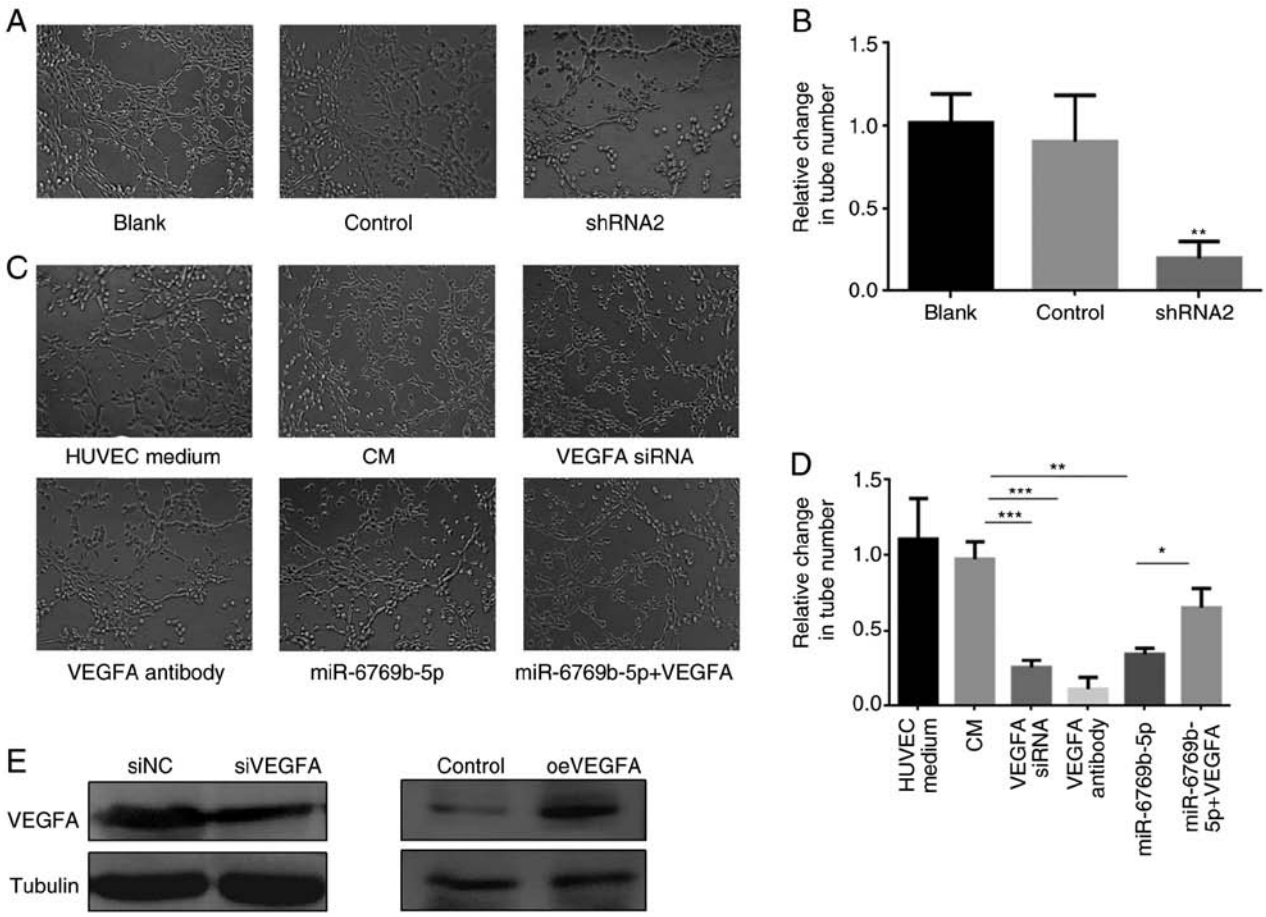

Figure 7. Effects of linc01105, miR-6769b-5p and VEGFA on angiogenesis. (A) HUVECs were cultured in CM from SH-SY5Y cells that were either untreated (blank), infected with control virus (control) or infected with linc01105-shRNA virus (shRNA2). (B) Quantification of tube formation ability from panel A. **P<0.01 compared with control. (C) HUVECs were cultured as follows: With HUVEC-specific media or with SH-SY5Y CM as positive control; with CM pre-treated with VEGFA antibody; with CM of SH-SY5Y cells transfected with a VEGFA-targeting siRNA; with CM of SH-SY5Y cells transfected with miR-6769b-5p mimics; and with CM of SH-SY5Y cells transfected with miR-6769b-5p mimics and VEGFA-overexpressing plasmid (n=3). Tube formation was observed after 6 h of culture using phase-contrast light microscopy. (D) Quantification of tube formation abilities from panel C. *P<0.05, **P<0.01 and ***P<0.005, with comparisons indicated by lines. (E) Validation of VEGFA knockdown and overexpression by siRNA and plasmid transfection, respectively. VEGFA, vascular endothelial growth factor A; HUVECs, human umbilical vein endothelial cells; CM, conditioned media; siRNA, small interfering RNA; shRNA, short hairpin RNA; NC, negative control; OE, overexpression.

and transfected into 293T cells. Luciferase activity was significantly increased following HIF-1α overexpression (Fig. 6D), confirming direct binding of HIF-1α with the promoter of linc01105. Finally, a CHIP-PCR assay also indicated that HIF-1α may bind directly with the promoter of linc01105 (Fig. 6E) and promote linc01105 transcription.

Linc01105 and miR-6769b-5p may participate in angiogenesis. HUVECs were used for tube-formation assays, in order to evaluate the angiogenesis potential. HUVECs were cultured with HUVEC-specific medium or the CM of SH-SY5Y cells. Silencing of linc01105 was demonstrated to inhibit endothelial cell tube formation (Fig. 7A and B). The tube formation ability of the CM was reduced by pretreatment of CM with VEGFA antibody, by VEGFA siRNA transfection in the SH-SY5Y cells, and by miR-6769b-5p overexpression by mimics transfection in the SH-SY5Y cells (Fig. 7C and D). The tube formation ability reduced by miR-6769b-5p overexpression was restored by VEGFA overexpression (Fig. 7C and D). Finally, silencing and overexpression of VEGFA were confirmed by western blotting (Fig. 7E).

Linc01105 gene targets. To explore more functions of linc01105, a CHIRP assay was performed to identify gene locations that are directly bound by linc01105. A protein interaction network was constructed using STRING for the linc01105-specific binding gene targets (after exclusion of targets identified by the negative control), revealing significant interactions between 20 genes (Fig. S1 and Table SI); among these genes were numerous ribosomal proteins and heat shock protein 90, which have been previously reported to be associated to tumorigenesis (27,28). Indeed, GO analysis demonstrated that linc01105 may impact a variety of biological processes. However, no KEGG pathway was found to be enriched, most likely due to low number of the 20 genes used as input in the analysis.

Discussion

Advanced NB patients are typically associated with a poor prognosis and frequent relapses despite treatment with a variety of therapies (29,30). Therefore, it is extremely important to identify novel biomarkers in order to improve the prognostic outcome of pediatric patients with NB (31). With

the development of genomics sequencing technologies, recent research has focused on lncRNAs (32,33). Increasing evidence suggests that lncRNAs participate in a number of biological processes and have important roles in human diseases, such as cancer (34,35).

Our previous study found that linc01105 was differentially expressed in NB and adjacent normal tissues through genome-wide lncRNA analysis (14). In addition, it was demonstrated that upregulation of linc01105 was correlated with NB INSS stage. In that previous study, the SK-N-BE(2)C cell line was used, which is a MYCN-amplification cell line; in the present study, the cell line SH-SY5Y was used, which is a non-MYCN amplification cell line, to further investigate the mechanism of linc01105 in NB. The present study focused on the molecular mechanism of linc01105. To explore the functions of linc01105, a nuclear-cytoplasmic fractionation was performed and the results revealed that linc01105 was mainly expressed in the cytoplasmic fraction. Subsequently, a loss-of-function assay was performed by linc01105 shRNA knockdown. Knockdown of linc01105 inhibited cell proliferation and promoted cell apoptosis. Notably, knockdown of linc01105 resulted in inhibition of migration and invasion. Furthermore, linc01105 silencing altered the expression of Bcl-2 family proteins and activated the p53/Caspase signaling pathway. These results indicated that linc01105 affected the apoptosis process via regulating Bcl-2 proteins and activating the p53/caspase signaling pathway.

One of the significant functions of lncRNAs, especially those located in the cell cytoplasm, is to bind with miRNAs, subsequently acting as a 'sponge' and inhibiting their expression (36-38). For example, in gastric cancer, linc01234 may have a role as a competing endogenous RNA to regulate core-binding factor subunit β expression by sponging miR-204-5p (36). Another study demonstrated that miR-29b-3p was directly inhibited by linc00511, which resulted in an increase in VEGFA expression in pancreatic ductal adenocarcinoma (39). Angiogenesis is crucial for tumor growth and is associated with tumor metastasis; notably, VEGFA is a major regulator of NB angiogenesis (40,41).

Bioinformatics analysis was performed to identify miRNAs that may bind with both linc01105 and VEGFA. The results revealed that miR-6769b-5p shared complementary binding sites with the VEGFA 3'UTR region and with linc01105 (924-948 nt region), which was confirmed by luciferase assay. RT-qPCR results indicated that miR-6769b-5p expression levels were lower in NB tissues compared with adjacent normal tissues. In addition, transfection with miR-6769b-5p mimics resulted in downregulation of VEGFA, while miR-6769b-5p inhibition resulted in upregulation of VEGFA expression. These findings suggested that linc01105, miR-6769b-5p and VEGFA mRNA constituted a competing endogenous RNA regulatory network. Silencing of linc01105 reduced the miR-6769b-5p competing adsorption and increased the levels of free miR-6769b-5p, thereby promoting the degradation of VEGFA by increasing binding to the 3'UTR region of VEGFA. Indeed, transfection with a miR-6769b-5p inhibitor suppressed VEGFA expression. By contrast, upregulation of linc01105 contributed to VEGFA upregulation via the competing endogenous RNA network. Of note, VEGFA knockdown had no influence on apoptosis but inhibited tumor migration (42,43). Therefore, the present study suggested that miR-6769b-5p may participate in NB tumorigenesis via interaction with VEGFA. The VEGF-mediated mechanism most likely has no effect on the p53/caspase signaling pathway, and the VEGFA network may only affect the migration phenotype of the linc01105 knockdown and not apoptosis.

The present study used the ALGGEN and JASPAR databases to predict transcription factors which may bind with the promoter of linc01105; among the predicted factors, HIF-1α was of particular interest, as high expression of HIF-1α has been widely reported to be associated with poor prognosis of NB (44,45). Over-expression of HIF-1α significantly promoted linc01105 expression levels. Furthermore, a luciferase assay confirmed that HIF-1α regulated the expression of linc01105 acting as a transcription factor and directly binding to its promoter. Additionally, the CHIRP assay identified 20 genes that directly bind with Linc01105, and which are potential candidates for future studies.

In conclusion, the present study demonstrated that linc01105 was significantly upregulated in NB tissues compared with normal tissues. Silencing of linc01105 resulted in the activation of the p53/caspase signaling pathway and the inhibition of NB cell proliferation, migration and invasion. In addition, silencing of linc01105 suppressed angiogenesis via miR-6769b-5p targeting of VEGFA. Taken together, these results suggested that the linc01105/p53/caspase pathway or the linc01105/miR-6769b-5p/VEGFA network may serve as candidate targets for future therapies for NB.

Acknowledgements

The authors wish to thank Ms Xia Wenjun and Mr Huang Jianbo (Fudan University, Shanghai, China), who provided kind assistance with all of the experiments.

Funding

This study received financial support from Shanghai Key Disciplines (grant no. 2017ZZ02022), National Natural Science Foundation of China (grant nos. 81771633 and 81572324) and Science Foundation of Shanghai (grant nos. 17411960600 and 15ZR1404200).

Availability of data and materials

The datasets used during the present study are available from the corresponding author upon reasonable request.

Authors' contributions

DK and YM designed the study. YM and MJ collected the data and performed experiments. LB and LX analyzed and interpreted the data. MD and DK were involved in critical reviewing of the manuscript. All authors read and approved the final manuscript.

Ethics approval and consent to participate

This study was approved by the Institute Research Ethics Committee at the Children's Hospital of Fudan University.

Informed consent was acquired from every patient's legal guardians.

Patient consent for publication

Not applicable.

Competing interests

The authors declare that they have no competing interests.

References

1. Mondal T, Juvvuna PK, Kirkeby A, Mitra S, Kosalai ST, Traxler L, Hertwig F, Wernig-Zorc S, Miranda C, Deland L, *et al*: Sense-antisense lncRNA pair encoded by locus 6p22.3 determines neuroblastoma susceptibility via the USP36-CHD7-SOX9 regulatory axis. Cancer Cell 33: 417-434 e7, 2018.
2. Duan C, Wang H, Chen Y, Chu P, Xing T, Gao C, Yue Z, Zheng J, Jin M, Gu W and Ma X: Whole exome sequencing reveals novel somatic alterations in neuroblastoma patients with chemotherapy. Cancer Cell Int 18: 21, 2018.
3. Li Z, Takenobu H, Setyawati AN, Akita N, Haruta M, Satoh S, Shinno Y, Chikaraishi K, Mukae K, Akter J, *et al*: EZH2 regulates neuroblastoma cell differentiation via NTRK1 promoter epigenetic modifications. Oncogene 37: 2714-2727, 2018.
4. Roy J and Mallick B: Investigating piwi-interacting RNA regulome in human Neuroblastoma. Genes Chromosomes Cancer 57: 339-349, 2018.
5. Singh N, Liu X, Hulitt J, Jiang S, June CH, Grupp SA, Barrett DM and Zhao Y: Nature of tumor control by permanently and transiently modified GD2 chimeric antigen receptor T cells in xenograft models of neuroblastoma. Cancer Immunol Res 2: 1059-1070, 2014.
6. Wang F, Yang H, Deng Z, Su Y, Fang Q and Yin Z: HOX antisense lincRNA HOXA-AS2 promotes tumorigenesis of hepatocellular carcinoma. Cell Physiol Biochem 40: 287-296, 2016.
7. Cheetham SW, Gruhl F, Mattick JS and Dinger ME: Long noncoding RNAs and the genetics of cancer. Brit J Cancer 108: 2419-2425, 2013.
8. Ding J, Xie M, Lian Y, Zhu Y, Peng P, Wang J, Wang L and Wang K: Long noncoding RNA HOXA-AS2 represses P21 and KLF2 expression transcription by binding with EZH2, LSD1 in colorectal cancer. Oncogenesis 6: e288, 2017.
9. Zheng H, Yang S, Yang Y, Yuan SX, Wu FQ, Wang LL, Yan HL, Sun SH and Zhou WP: Epigenetically silenced long noncoding-SRHC promotes proliferation of hepatocellular carcinoma. J Cancer Res Clin Oncol 141: 1195-1203, 2015.
10. Dong R, Liu GB, Liu BH, Chen G, Li K, Zheng S and Dong KR: Targeting long non-coding RNA-TUG1 inhibits tumor growth and angiogenesis in hepatoblastoma. Cell Death Dis 7: e2278, 2016.
11. Wu L, Murat P, Matak-Vinkovic D, Murrell A and Balasubramanian S: Binding interactions between long noncoding RNA HOTAIR and PRC2 proteins. Biochemistry 52: 9519-9527, 2013.
12. Tsai KW, Lo YH, Yeh CY, Chen YZ, Hsu CW, Chen WS and Wang JH: Linc00659, a long noncoding RNA, acts as novel oncogene in regulating cancer cell growth in colorectal cancer. Mol Cancer 17: 72, 2018.
13. Nallasamy P, Chava S, Verma SS, Mishra S, Gorantla S, Coulter DW, Byrareddy SN, Batra SK, Gupta SC and Challagundla KB: PD-L1, inflammation, non-coding RNAs, and neuroblastoma: Immuno-oncology perspective. Semin Cancer Biol 52: 53-65, 2018.
14. Tang W, Dong K, Li K, Dong R and Zheng S: MEG3, HCN3 and linc01105 influence the proliferation and apoptosis of neuroblastoma cells via the HIF-1α and p53 pathways. Sci Rep 6: 36268, 2016.
15. Russell MR, Penikis A, Oldridge DA, Alvarez-Dominguez JR, McDaniel L, Diamond M, Padovan O, Raman P, Li Y, Wei JS, *et al*: CASC15-S is a tumor suppressor lncRNA at the 6p22 neuroblastoma susceptibility locus. Cancer Res 75: 3155-3166, 2015.
16. Liu PY, Erriquez D, Marshall GM, Tee AE, Polly P, Wong M, Liu B, Bell JL, Zhang XD, Milazzo G, *et al*: Effects of a novel long noncoding RNA, lncUSMycN, on N-Myc expression and neuroblastoma progression. J Natl Cancer Inst 106: pii: dju113, 2014.
17. Li D, Wang X, Mei H, Fang E, Ye L, Song H, Yang F, Li H, Huang K, Zheng L and Tong Q: Long noncoding RNA pancEts-1 promotes neuroblastoma progression through hnRNPK-mediated β-catenin stabilization. Cancer Res 78: 1169-1183, 2018.
18. Liang L, Xu J, Wang M, Xu G, Zhang N, Wang G and Zhao Y: LncRNA HCP5 promotes follicular thyroid carcinoma progression via miRNAs sponge. Cell Death Dis 9: 372, 2018.
19. Zhang ZK, Li J, Guan D, Liang C, Zhuo Z, Liu J, Lu A, Zhang G and Zhang BT: A newly identified lncRNA MAR1 acts as a miR-487b sponge to promote skeletal muscle differentiation and regeneration. J Cachexia Sarcopenia Muscle 9: 613-626, 2018.
20. Livak KJ and Schmittgen TD: Analysis of relative gene expression data using real-time quantitative PCR and the 2(-Delta Delta C(T)) method. Methods 25: 402-408, 2001.
21. Zhong J, Wang H, Chen W, Sun Z, Chen J, Xu Y, Weng M, Shi Q, Ma D and Miao C: Ubiquitylation of MFHAS1 by the ubiquitin ligase praja2 promotes M1 macrophage polarization by activating JNK and p38 pathways. Cell Death Dis 8: e2763, 2017.
22. Morelli C, Garofalo C, Sisci D, del Rincon S, Cascio S, Tu X, Vecchione A, Sauter ER, Miller WH Jr and Surmacz E: Nuclear insulin receptor substrate 1 interacts with estrogen receptor alpha at ERE promoters. Oncogene 23: 7517-7526, 2004.
23. Chu C, Quinn J and Chang HY: Chromatin isolation by RNA purification (ChIRP). J Vis Exp 25: pii: 3912, 2012.
24. Gowda Saralamma VV, Lee HJ, Raha S, Lee WS, Kim EH, Lee SJ, Heo JD, Won C, Kang CK and Kim GS: Inhibition of IAP's and activation of p53 leads to caspase-dependent apoptosis in gastric cancer cells treated with Scutellarein. Oncotarget 9: 5993-6006, 2017.
25. Ehrnhoefer DE, Skotte NH, Ladha S, Nguyen YT, Qiu X, Deng Y, Huynh KT, Engemann S, Nielsen SM, Becanovic K, *et al*: p53 increases caspase-6 expression and activation in muscle tissue expressing mutant huntingtin. Hum Mol Genet 23: 717-729, 2014.
26. Guo XX, Li Y, Sun C, Jiang D, Lin YJ, Jin FX, Lee SK and Jin YH: p53-dependent fas expression is critical for ginsenoside Rh2 triggered caspase-8 activation in HeLa cells. Protein Cell 5: 224-234, 2014.
27. Rong B and Yang S: Molecular mechanism and targeted therapy of Hsp90 involved in lung cancer: New discoveries and developments (Review). Int J Oncol 52: 321-336, 2018.
28. Gao C, Peng YN, Wang HZ, Fang SL, Zhang M, Zhao Q and Liu J: Inhibition of heat shock protein 90 as a novel platform for the treatment of cancer. Curr Pharm Des 25: 849-855, 2019.
29. Chen Q, Deng R, Zhao X, Yuan H, Zhang H, Dou J, Chen R, Jin H, Wang Y, Huang J and Yu J: Sumoylation of EphB1 suppresses neuroblastoma tumorigenesis via inhibiting PKCγ activation. Cell Physiol Biochem 45: 2283-2292, 2018.
30. Batzke K, Büchel G, Hansen W and Schramm A: TrkB-target galectin-1 impairs immune activation and radiation responses in neuroblastoma: Implications for tumour therapy. Int J Mol Sci 19: pii: E718, 2018.
31. Szemes M, Greenhough A, Melegh Z, Malik S, Yuksel A, Catchpoole D, Gallacher K, Kollareddy M, Park JH and Malik K: Wnt signalling drives context-dependent differentiation or proliferation in neuroblastoma. Neoplasia 20: 335-350, 2018.
32. Yang S, Xu J and Zeng X: A six-long non-coding RNA signature predicts prognosis in melanoma patients. Int J Oncol 52: 1178-1188, 2018.
33. Yamada A, Yu P, Lin W, Okugawa Y, Boland CR and Goel A: A RNA-Sequencing approach for the identification of novel long non-coding RNA biomarkers in colorectal cancer. Sci Rep 8: 575, 2018.
34. Huang T, Wang M, Huang B, Chang A, Liu F, Zhang Y and Jiang B: Long noncoding RNAs in the mTOR signaling network: Biomarkers and therapeutic targets. Apoptosis 23: 255-264, 2018.
35. Janakiraman H, House RP, Gangaraju VK, Diehl JA, Howe PH and Palanisamy V: The long (lncRNA) and short (miRNA) of It: TGFβ-mediated control of RNA-binding proteins and noncoding RNAs. Mol Cancer Res 16: 567-579, 2018.
36. Chen X, Chen Z, Yu S, Nie F, Yan S, Ma P, Chen Q, Wei C, Fu H, Xu T, *et al*: Long noncoding RNA LINC01234 functions as a competing endogenous RNA to regulate CBFB expression by sponging miR-204-5p in gastric cancer. Clin Cancer Res 15: 2002-2014, 2018.

37. Liu XH, Sun M, Nie FQ, Ge YB, Zhang EB, Yin DD, Kong R, Xia R, Lu KH, Li JH, *et al*: Lnc RNA HOTAIR functions as a competing endogenous RNA to regulate HER2 expression by sponging miR-331-3p in gastric cancer. Mol Cancer 13: 92, 2014.
38. Xie CR, Wang F, Zhang S, Wang FQ, Zheng S, Li Z, Lv J, Qi HQ, Fang QL, Wang XM and Yin ZY: Long noncoding RNA HCAL facilitates the growth and metastasis of hepatocellular carcinoma by acting as a ceRNA of LAPTM4B. Mol Ther Nucleic Acids 9: 440-451, 2017.
39. Zhao X, Liu Y, Li Z, Zheng S, Wang Z, Li W, Bi Z, Li L, Jiang Y, Luo Y, *et al*: Linc00511 acts as a competing endogenous RNA to regulate VEGFA expression through sponging hsa-miR-29b-3p in pancreatic ductal adenocarcinoma. J Cell Mol Med 22: 655-667, 2018.
40. Weng WC, Lin KH, Wu PY, Ho YH, Liu YL, Wang BJ, Chen CC, Lin YC, Liao YF, Lee WT, *et al*: VEGF expression correlates with neuronal differentiation and predicts a favorable prognosis in patients with neuroblastoma. Sci Rep 7: 11212, 2017.
41. Fakhari M, Pullirsch D, Paya K, Abraham D, Hofbauer R and Aharinejad S: Upregulation of vascular endothelial growth factor receptors is associated with advanced neuroblastoma. J Pediatr Surg 37: 582-587, 2002.
42. Weng WC, Lin KH, Wu PY, Lu YC, Weng YC, Wang BJ, Liao YF, Hsu WM, Lee WT and Lee H: Calreticulin regulates VEGF-A in neuroblastoma cells. Mol Neurobiol 52: 758-770, 2015.
43. Kaneko S, Ishibashi M and Kaneko M: Vascular endothelial growth factor expression is closely related to irinotecan-mediated inhibition of tumor growth and angiogenesis in neuroblastoma xenografts. Cancer Sci 99: 1209-1217, 2008.
44. Yin CP, Guan SH, Zhang B, Wang XX and Yue SW: Upregulation of HIF-1α protects neuroblastoma cells from hypoxia-induced apoptosis in a RhoA-dependent manner. Mol Med Rep 12: 7123-7131, 2015.
45. Westerlund I, Shi Y, Toskas K, Fell SM, Li S, Surova O, Södersten E, Kogner P, Nyman U, Schlisio S and Holmberg J: Combined epigenetic and differentiation-based treatment inhibits neuroblastoma tumor growth and links HIF2α to tumor suppression. Proc Natl Acad Sci USA 114: E6137-E6146, 2017.